frontiers | Frontiers in Mechanical Engineering

TYPE Original Research
PUBLISHED 02 November 2023
DOI 10.3389/fmech.2023.1215352

OPEN ACCESS

EDITED BY
Gabriele Di Blasio,
National Research Council (CNR), Italy

REVIEWED BY
Ali Erdemir,
Texas A and M University, United States
Henara Lillian Costa,
Federal University of Rio Grande, Brazil
Wenbo Wang,
Oak Ridge National Laboratory (DOE), United States

*CORRESPONDENCE
Peter M. Lee,
peter.lee@swri.org

RECEIVED 01 May 2023
ACCEPTED 09 October 2023
PUBLISHED 02 November 2023

CITATION
Lee PM, Sanchez C, Frazier C, Velasquez A and Kostan T (2023), Tribological evaluation of electric vehicle driveline lubricants in an electrified environment.
Front. Mech. Eng 9:1215352.
doi: 10.3389/fmech.2023.1215352

Tribological evaluation of electric vehicle driveline lubricants in an electrified environment

Peter M. Lee*, Carlos Sanchez, Cole Frazier, Andrew Velasquez and Travis Kostan

Tribology Research and Evaluations, Fuels and Lubricants Division, Southwest Research Institute, San Antonio, TX, United States

Electrification continues to permeate the automotive industry, with future projections showing an exponential growth in the market share for both light and heavy-duty applications. Existing test methods for automotive applications were developed to model internal combustion engine vehicles and drivelines and are not appropriate for electric drivelines that experience stray electric currents. Tribometers can be used to evaluate friction and wear on modeled surfaces simulating in-vehicle operation. In this work, a commercially available tribometer was modified to isolate an electrical input into a tribological contact. After necessary modifications to the tribometer, a test matrix was completed for investigating different temperatures, load conditions, speed conditions, voltage input types, frequencies of AC signal, and shapes of AC signal. These parameters were tested on three lubricants—two typical automatic transmission fluid formulations and gear oil used in differential applications. Friction was measured throughout the tests, and wear scar width was measured at the end of each test. Results indicated that temperature, DC voltage, AC frequency, lubricant, and test profile had statistically significant differences in wear scar width. For electrical parameters, AC frequency produced different results from DC voltage when no voltage was applied. This significance applied to only one lubricant, with the other two lubricants having mixed results.

KEYWORDS

electric vehicles, electrification, tribology, wear, fluids

1 Introduction

The primary mode of propulsion for most modern electric vehicles derives from a large, brushless AC induction or a permanent magnet motor. This motor runs on energy from large on-board battery packs. An inverter considers the DC voltage output from the batteries and converts it into the necessary three-phase AC power required to operate the motor. Using high carrier frequencies to switch the DC power on and off, the inverter simulates AC power by utilizing a pulse-width-modulated (PWM) signal to approximate the curve of a sine wave (He et al., 2019).

Due to the presence of a large AC motor, rotating components are exposed to shaft voltages and the large electric field inherent with such high voltages. Shaft voltage generation is not a new concept—frictional-based electrostatics and manufacturing-based magnetic field asymmetry are both historical phenomena causing motor shaft voltage generation (Hadden et al., 2016). A relatively new effect is caused by the high switching frequencies of the inverter. Faster switching inverters provide advantages to system efficiency by mimicking

a more exact sine wave. However, the speed at which the voltage changes causes local voltage spikes on the shaft (Somani et al., 2012; Tischmacher et al., 2010). After these stray voltages are generated, there are numerous grounding paths available. The exact grounding location is highly systematic and operationally dependent (Evo et al., 2021).

While grounding through the load side is theoretically possible, a more common grounding path involves flow through the electric motor's deep-groove ball bearings, which support the rotor to motor housing. Due to their proximity toward the origin point of stray currents, motor bearings are widely considered the rotating component that are most at risk to potentially damaging current flow. The electric potential across the bearing builds until the voltage exceeds the dielectric strength of the thin film of lubricant separating the ball from the bearing raceway. Once breakdown of voltage is achieved, a rapid transfer of current across the bearing tends to result in surface damage (Juan et al., 2022; Harder et al., 2022; Suzumura, 2016). There are no commercially available tribometers at this time that can reproduce this electrified condition, hence requiring the full electric drivetrain for such studies.

This work aimed to convert a tribometer to run test samples and oils in an electrified environment representative of an electric vehicle driveline as well as an initial investigation into the effect of this electrified environment on the friction and wear of components, while operating with electric vehicle driveline fluids. This paper reports the wear, and a future paper will report the friction results. In addition, we are currently in the process of electrifying other tribometers and will be reporting these results in future papers.

2 Materials and methods

2.1 Test rig

Modifications to an existing commercial tribometer were performed. The selected instrument enables motion studies applicable to different types of contacts, and we have considerable experience adapting this tribometer for testing. Due to the high speeds and linear contacts of motor bearings in electric vehicles, the block-on-ring (BOR) wear test methodology was selected to replicate those conditions. This test method comprised a stationary block, loaded against a rotating ring as per ASTM G77. (ASTM, 2022). The standard BOR set up was not capable of studying wear between the block and ring in an electrified environment as would be seen in the motor bearings of electric vehicles, so significant modifications were undertaken.

One key component for BOR testing is the reservoir for holding the lubricant. As the ring rotates, a film of lubricant becomes entrained on the ring, creating a lubricant film between the block and ring test components. The typical BOR test instrument is made from steel parts which, if electrified, would not accurately measure electrical conditions between the block and ring, across the lubricant. In addition, applying an electrical potential will damage some parts and electronics of the instrument. Therefore, a design which allowed electrical isolation of the BOR test stand from the test components was needed to ensure the potential would flow only across the block and ring components, through the lubricant film. The materials used in the design also needed to be heat resistant to withstand elevated test temperatures up to 120°C. Figure 1 displays typical BOR testing, prior to major modification.

For the purpose of electric vehicle fluid testing, the majority of tests were run at high rotational speeds. Due to the configuration of the parts and the fluid reservoir, the test lubricant flows more erratically inside the chamber as the ring increases speed. This leads to lubricant loss near the top and side openings of the reservoir. These losses hinder the lubricant from forming a consistent film between the block and ring interfaces, resulting in a thinner and non-uniform film thickness. Thus, careful design was required to prevent lubricant loss. To maintain the lubricant quality within the BOR reservoir, a heated sump with an additional lubricant was externally pumped into the reservoir. This supply of lubricant was heated with resistive heating elements and, therefore, must also be isolated from the electrified environment to prevent the disruption of the electrical properties within the BOR fixture. Isolating the heated reservoir from the BOR reservoir also ensured that no magnetic field was introduced to the test components. The pump must also be able to function at the higher lubricant temperatures without affecting the flow rate going to the BOR reservoir. Therefore, a heat exchanger style system with a peristaltic pump was designed to meet the requirements. The final design of BOR test assembly is shown in Figure 2.

2.2 Test fluids and parts

Three lubricants were used for wear evaluation, following the completion of the electrically isolated BOR design. The test lubricants were MERCON® ULV, DEXRON®-VI, and market J2360 automotive gear oil (AGO). The MERCON® ULV and DEXRON®-VI are common oils used in automatic transmissions and are of a lower viscosity compared to AGO which is a common oil used in rear differential applications. The viscosity of the lubricants are 4.5 cSt for MERCON® ULV, 6 cSt for DEXRON®-VI, and 11.4 cSt for AGO, all at 100°C.

To maintain continuity of tests, block and ring samples that conformed to the ASTM G77 standards were chosen (ASTM, 2022). The ring samples were standard ASTM G-77 Falex F-S10 rings made of SAE #4620 steel with a hardness of 58–63 HRC and surface roughness between 6–12 µin rms. The block samples were also supplied by Falex and conformed to the same standard as the rings with similar hardness but made from SAE-O1 steel and had a surface roughness of 0.102–0.203 µm rms. Before testing, the samples were sonicated in hexane for 20 min at 30°C to remove any oil and debris. The samples were then weighed on a GR-300 scale with a resolution of 0.0001 g. After testing, the samples followed the same rinsing and weighing process as performed during initial preparation to determine mass loss/gain after testing.

2.3 Test parameters

The first fluid tested in this study was ULV. When creating the ULV test matrix, it was decided that it would be best to run a wider

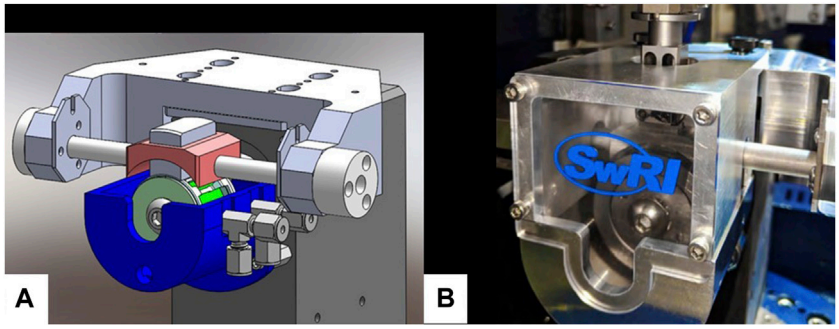

FIGURE 1
Computer-aided design model of the Block-on-Ring test configuration for UMT **(A)** and the physical implementation of the same model **(B)**.

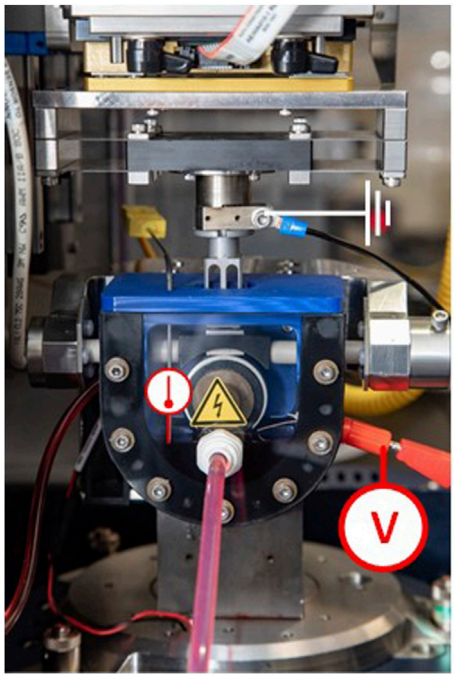

FIGURE 2
Full assembly of the EV Block-on-Ring design including applied potential locations and temperature measurement.

array of test conditions to understand which one made significant impacts. Current amplitude was restricted to 2 amps for DC voltage and 4 amps for AC voltage. Frequency for AC voltages was also restricted to 1 kHz and 20 kHz for the two different wave forms. Multiple temperatures were included in the test matrix: 25, 40, 60, 80, 100, and 120°C.

The electric conditions to which the BOR environment was subjected were selected to represent voltages and amplitudes considered extreme in an EV motor–gearbox system, as measured at the Southwest Research Institute (SwRI). These conditions were chosen to see if electrification affected friction and wear, as well as to accelerate the testing. As results were obtained, and as more research was undertaken into electric vehicle drivelines, these test conditions were refined.

Two different test protocols were created for the BOR test, one with constant load and variable speed and another with constant speed and variable load. The variable load profile maintained a constant speed of 1,000 rpm throughout the test and increased the load by 5N every 5 minutes until a maximum of 90 N was reached, with the initial force starting at 15 N. The variable speed profile maintained a constant load of 90 N throughout the test and increased the speed by 500 rpm every 5 minutes until a maximum of 8,000 rpm was reached, with the initial speed starting at 500 rpm. Running two different profiles offers the opportunity to determine which physical characteristics predominately contributed to wear mechanisms. These test parameters allow the evaluation of an electrified contact at a variety of lubrication regimes, from boundary to hydrodynamic. Using Hamrock's minimum film thickness equation for line contacts (Hamrock et al., 2004), the lowest lamda ratio achieved at the minimum speed, maximum load, and thickest viscosity was approximately 0.4. Conversely, the highest lamda ratio achieved at the maximum speed, nominal load, and thinnest viscosity was approximately 64.

The temperature of the lubricant was also varied in the test matrix. Temperature ranged from 25°C to 120°C. This range was chosen based on data collected during a fluid-aging study in a battery electric vehicle, also performed at SwRI. It is known that temperate affects lubricant viscosity, which will alter the performance of the fluid, thereby impacting friction and wear behavior. It was not known how the presence of an electric field would change lubricant viscosity with respect to the temperature in the system.

2.4 Wear measurements

The wear on the block was examined using a Keyence VR-5000 series imaging system. The block wear scar width was measured at three locations and then averaged to find the overall scar width as shown in Figure 3. Wear scar severity was determined by the average width of the wear scar. Only tests with a wear scar coefficient of variance (CoV) of less than 10% were deemed to be valid tests, as per ASTM G 77 (ASTM, 2022). The rings were also imaged, but no analytical measurements were taken since it is not standard for the ring wear to be measured.

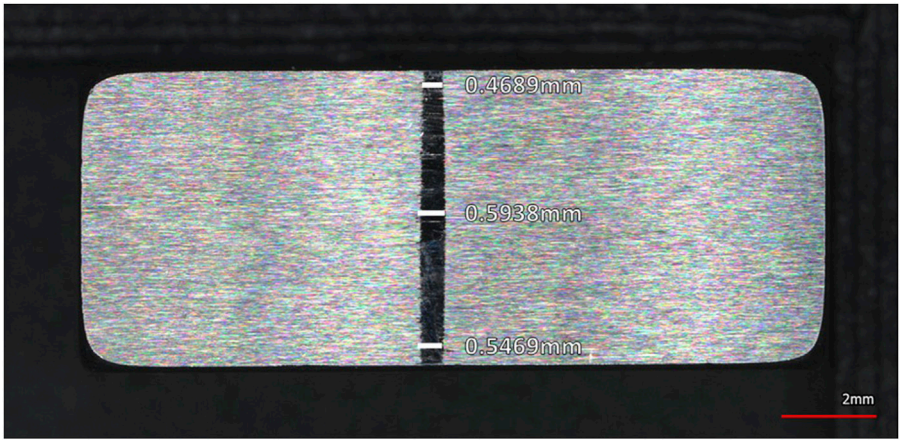

FIGURE 3
Example of wear scar measurements made for the block.

TABLE 1 List of predictor variables.

Predictor variable	Predictor type	Range/levels
Temperature [°C]	Continuous	25–120
Fluid	Categorical	MERCON ULV, DEXRON®-VI, and AGO
Voltage [V]	Categorical	0 (none), DC, sine wave, and PWM
Frequency [kHz]	Categorical	0, 1, and 20
Variable speed/load	Categorical	Speed and load

TABLE 2 Initial variable screening using a bootstrap forest.

Predictor	Contribution	Portion	Rank
Variable [speed/load]	3.05417	0.3418	1
Temperature [°C]	2.81835	0.3154	2
Fluid	1.50116	0.1680	3
Frequency [kHz]	0.85513	0.0957	4
Voltage [V]	0.70748	0.0792	5

3 Results and discussion

The electrification of a tribo-test is a new area, and therefore, a lot of unknowns persist. A large test matrix was initially designed to account for all possible scenarios. Only one lubricant was subjected to the large matrix of 29 tests, MERCON® ULV. After reviewing the results for tests using the ULV oil, it was found that certain conditions generated more wear on the block than others. After data analysis, a new, reduced test matrix was designed for testing DEXRON®-VI and AGO oils based on variables that resulted in statistically significant changes in wear.

Initial predictor screening was conducted using a bootstrap forest partition model. Table 1 shows the predictor variables, and results are shown in Table 2. Screening indicated that temperate and whether the test was a variable speed or variable load test were likely to be the most important predictors of average scar width.

Many statistical models were considered, and some of them required that the model residuals follow a normal distribution to perform statistical tests to determine predictor significance. It is very common when modeling a wear component that a natural log or square root transformation will satisfy this requirement. A Box–Cox analysis was performed on a standard least square regression model using just the top two factors from variable screening. Box–Cox indicated that a natural log transformation would be appropriate for the data. Therefore, all the models considered were built to predict the natural log of the average scar width. A plot of the natural log of the average scar width vs. temperature, with separate columns for variable speed and load tests, colored by fluid, is shown in Figure 4.

The lines shown are moving average lines. It can be seen from Figure 4 that the variable speed tests in general have greater average scar width compared to the variable load tests. It is also apparent that only for variable speed tests does wear increase with temperature. In general, the variable speed tests were found to be more severe than the variable load tests. This is because a high load was applied throughout the varied speed test profile, whereas the variable load test profile used a more moderate speed. Thus, conditions in the speed test were on average more severe. Motor bearings used in electric vehicle applications operate at high speeds, with EV motors on the road today operating up to 20,000 rpm. These high-speed conditions are relevant to EV applications. The BOR test assembly is

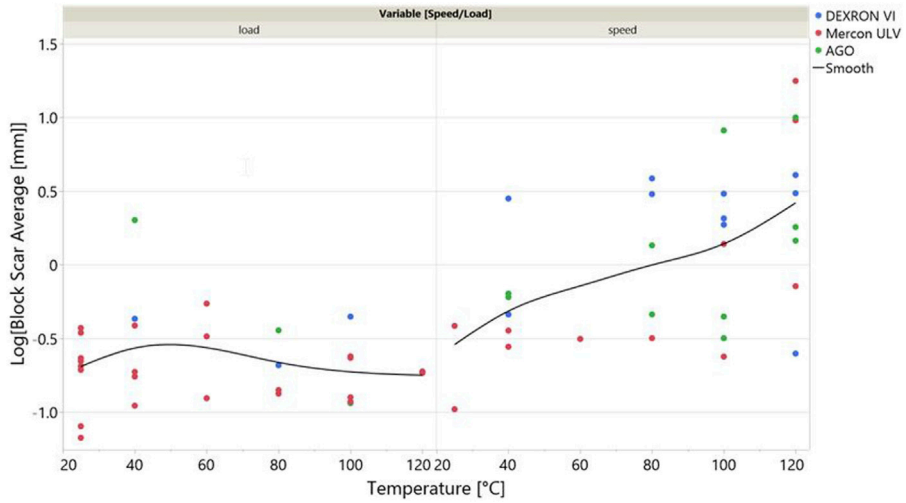

FIGURE 4
Log (block scar avg.) vs. temperature by variable speed/load, colored by fluid.

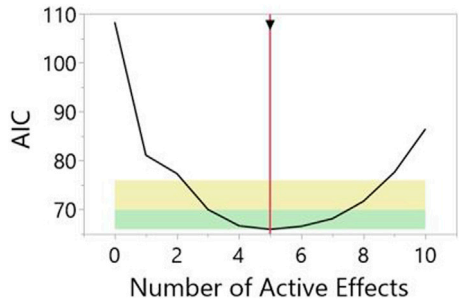

FIGURE 5
Number of active model effects based on minimum AIC.

specifically designed to replicate the ball bearing contact, so results in the bench test would be expected to generally apply to in-field motor bearings. As for fluid differences, for the variable speed tests, there is a bit of separation with DEXRON®-VI having the highest average scar width, followed by AGO and then MERCON® ULV.

Many different statistical models were considered in the analysis, including standard least squares regression, penalized regression, bootstrap forest, and support vector machines. These models differ in terms of complexity, assumptions, and interpretability. In the end, the prediction capability was very similar across all models, and therefore, the best model was chosen based on interpretability, which is best for standard least squares regression.

To determine the best least squares regression model, the best subset variable selection process was utilized. Candidate variables included the main effects of variables along with all two-way interactions. The process used determined the best one-variable model among all possible choices based on minimizing the Akaike information criterion (AIC), which is an estimator of prediction error. Next, the process determined the best two-variable model based on minimum AIC, and it was continued until determining the best 10-variable model. Unlike an R-squared metric which is guaranteed to increase with additional variables, this process is robust to overfitting. Figure 5 shows that the optimal number of model effects is five.

The analysis of variance (ANOVA) table showing the best five-factor model is shown in Table 3. The important main effects are fluid and whether the test was of variable speed or load. Additionally, there is an effect for temperature which is dependent on variable speed/load designation (as seen in Figure 4) as well as fluid. Finally, there is a frequency effect dependent on fluid.

First, we begin with the fluid effect, and Figure 6 provides a least square (LS) means plot of the three fluids with 95% confidence intervals. Table 4 follows Tukey's multiple comparison tests which indicate that the difference between DEXRON®-VI and MERCON® ULV is statistically significant, but the other two pairwise comparisons are not. Back-transforming the LS mean of the two statistically different fluids to their original units gives a scar width of 0.97 mm for DEXRON®-VI and 0.62 mm for MERCON® ULV, which means that DEXRON®-VI produced a wear scar increase of roughly 50% over MERCON® ULV.

Similar LS means plots with a subsequent *t*-test table are shown for the variable speed/load factor in Figure 7 and Table 5. Based on the estimated difference of 0.5358 in transformed units, using a baseline of 0.50 mm for a variable load test, we would expect a change to a variable speed test to increase the average scar width to 0.85 mm, a 70% increase.

The temperature effect was shown to be present for the variable speed testing only and was also deemed to be fluid dependent. Therefore, using the estimated coefficients for each fluid from the model, Table 6 shows what an expected change would be from a baseline measurement of 0.50 mm changing from 20°C to 120°C.

All factors discussed to this point were highly statistically significant, with *p*-values <0.01. The final factor was marginally significant, with a *p*-value of 0.05. This factor was the interaction Frequency*Fluid, meaning that there were differences in how the fluids responded to frequency levels. A plot of the Ln (scar width average) vs. frequency is shown in Figure 8.

TABLE 3 ANOVA table for the prediction model used.

Source	DF	Sum of squares	F ratio	Prob > F
Fluid	2	1.516	5.922	0.0050*
Variable [speed/load]	1	3.298	25.761	<.0001*
Variable [speed/load]*temperature [°C]	1	2.452	19.154	<.0001*
Temperature [C]*fluid	2	1.640	6.407	0.0034*
Fluid*frequency [kHz]	4	1.304	2.547	0.0510

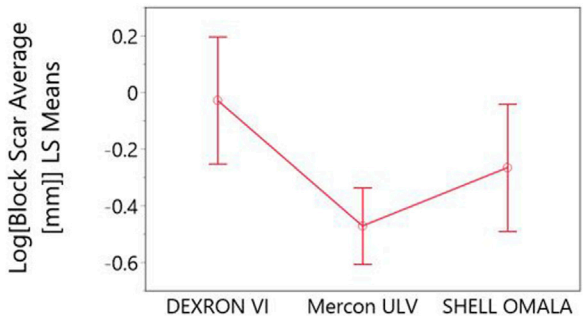

FIGURE 6
Fluid least square means plot with 95% confidence intervals.

TABLE 4 Tukey multiple comparison tests between fluids.

Level	- Level	Difference	*p*-value
DEXRON®-VI	MERCON ULV	0.4432	0.0040*
DEXRON®-VI	AGO	0.2374	0.2972
AGO	MERCON ULV	0.2057	0.2688

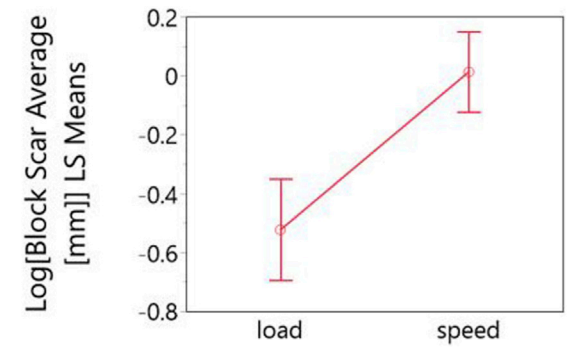

FIGURE 7
Variable load/speed least square means plot with 95% confidence intervals.

It can be difficult to examine the effect of a particular factor from a raw data x–y plot when multiple significant factors are present. Since frequency does not interact when any variables other than fluid in our model, we can pick any one combination of these other factors and examine the predicted marginal effect of frequency after accounting for all other factors. Figure 9 shows the predicted change in average scar width at 80°C for variable speed testing. It appears from this plot that DEXRON®-VI shows increased wear whenever the alternating current is applied, whether at the lower or at the higher frequency. MERCON® ULV and AGO show a lower predicted scar width and no effect of frequency except for an increase in predicted wear for AGO at 0 frequency. Based on the raw data plot in Figure 8, this appears to be driven by two data points with higher scar width. Should these points have had any unknown operational anomalies making them invalid or outliers, this predicted effect would not be present.

TABLE 5 T-test of variable speed vs. variable load.

Level	- Level	Difference	*p*-value
Speed	Load	0.5358	<.0001*

4 Conclusion

An electrically isolated BOR test configuration was designed around a commercially available tribometer in an effort to understand the effects that applied electrical potential has on typical EV driveline fluids. A test matrix was developed to investigate the wear on the block component as related to temperature, rotational speed, contact pressure, DC voltage, AC frequency, and lubricant type. Through subjecting one lubricant through the entire 29 test matrix, it was determined that certain factors had high impacts on wear. After reducing the matrix, two more lubricants were evaluated. Overall, the results demonstrated that some conditions have the potential to increase the average wear scar on the block by 50%–70%

The parameters that had a significant effect on wear were speed and load. Results indicated that variable speed tests at constant load produced higher wear compared to variable load tests at constant speed. The fluid type also had a significant effect on wear. DEXRON®-VI produced more wear than MERCON® ULV. Additionally, for DEXRON® -VI, tests run at no applied current to those run with either a DC or AC current at 1 kHz or 20 kHz frequency resulted in a statistically significant block wear.

The temperature of the fluid had the highest impact when running at the low and high extremes of 25°C and 120°C, respectively. The mid-range temperatures of 40°C, 60°C, 80°C, and 100°C did not have a

TABLE 6 Predicted change in average scar width by fluid when changing the temperature from 20°C to 120°C, the variable speed test only.

Fluid	Change in Ln (scar width) 20 C–120 C	Change in average scar width using a baseline of 0.50 mm
DEXRON®-VI	0.0815	0.54
AGO	0.6483	0.96
Mercon ULV	1.3045	1.84

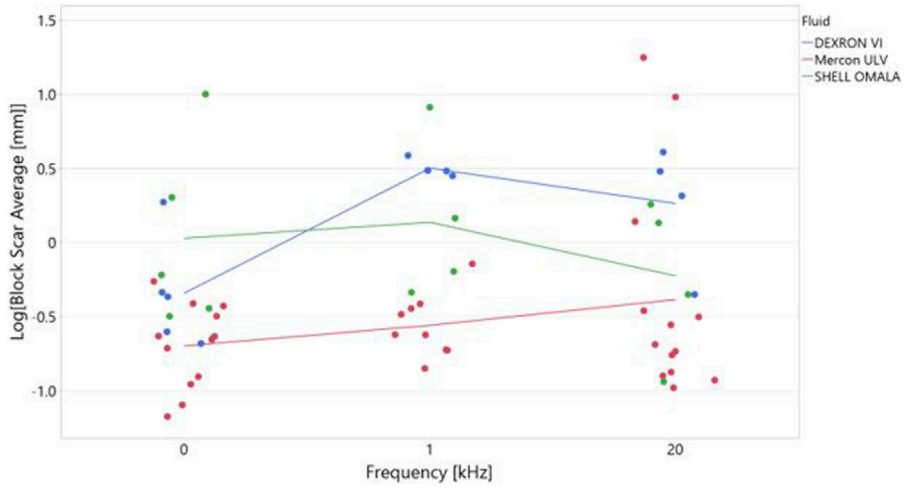

FIGURE 8
Log (scar width avg.) vs. frequency by fluid.

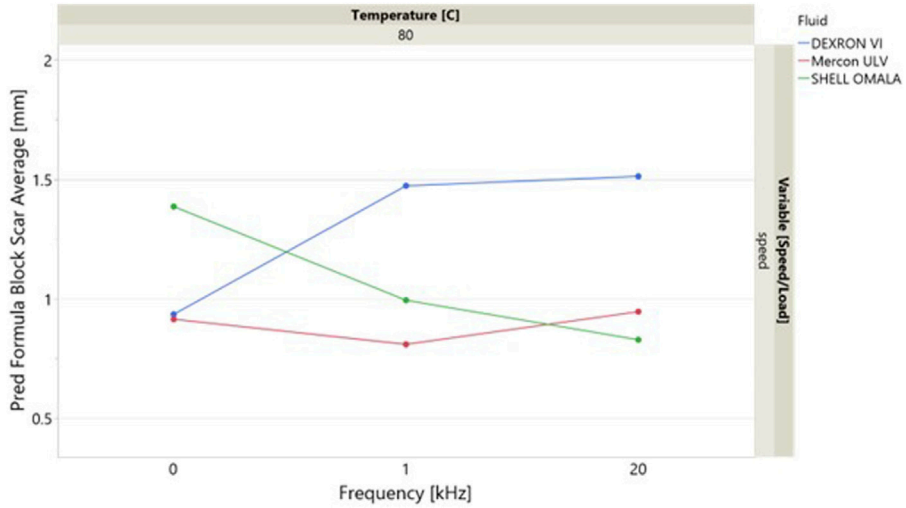

FIGURE 9
Predicted scar avg. vs. frequency by fluid at 80°C for variable speed tests.

significant impact on wear. However, this effect was highly fluid dependent and only evident for the variable speed and constant load tests. Block wear for DEXRON®-VI was independent of temperature, exhibiting no change, while AGO showed a 100% increase and MERCON® ULV showed a 268% increase when running at 125°C versus 25°C.

Based on the statistical analysis presented previously, electrification resulted in varied wear on the block and ring components under some conditions. Overall, DC voltage produced different wear results than AC frequency. The impact of AC frequency, 1 kHz versus 20 kHz, was the only electrical parameter to show a statistically significant difference in wear.

However, the significance was only seen for DEXRON®-VI. The other fluids did not exhibit a statistically significant difference in block wear for electrified versus non-electrified testing.

The work presented herein represents early research in the field of EV tribology testing. This study showed that the presence of an electrical voltage and/or current has the possibility to increase wear on tribo pairs. However, the magnitude of wear is dependent on the lubricant type. This implies that there is potential to utilize an electrified tribometer to develop lubricants specifically for electric vehicle drivelines, thereby optimizing fluids and materials for improved performance.

Data availability statement

The datasets presented in this article are not readily available because of Internal SwRI R&D. Requests to access the datasets should be directed to peter.lee@swri.org.

Author contributions

CF was the project manager for the work. CS performed design modifications and initial shakedown testing. AV completed the majority of testing. PL provided guidance and oversight on technical issues. TK performed statistical analysis on raw data to draw primary conclusion. All authors contributed to the article and approved the submitted version.

Funding

Funding was provided by the Southwest Research Institute's internal research and development program.

Conflict of interest

The authors declare that the research was conducted in the absence of any commercial or financial relationships that could be construed as a potential conflict of interest.

Publisher's note

All claims expressed in this article are solely those of the authors and do not necessarily represent those of their affiliated organizations, or those of the publisher, the editors, and the reviewers. Any product that may be evaluated in this article, or claim that may be made by its manufacturer, is not guaranteed or endorsed by the publisher.

References

ASTM (2022). *Standard test method for ranking of resistance of materials to sliding wear using block-on-ring wear test*. West Conshohocken, PA, USA: ASTM International.

Evo, M. T., Alzamora, A. M., Zaparoli, I. O., and de Paula, H. (2022). "Inverter-Induced bearing currents: a thorough study of the cause-and-effect chains," in Proceedings of the IEEE Industry Applications Magazine, Vancouver, BC, Canada, October, 2021.

Hadden, T., Jiang, J. W., Bilgin, B., Yang, Y., Sathyan, A., Dadkhah, H., et al. (2016). "A review of shaft voltages and bearing currents in EV and HEV motors," in Proceedings of the IECON 2016-42nd Annual Conference of the IEEE Industrial Electronics Society, Florence, Italy, October, 2016, 1578–1583.

Hamrock, B. J., Schmid, S. R., and Jacobson, B. O. (2004). *Fundamentals of fluid film lubrication*. Boca Raton, Florida, United States: CRC Press.

Harder, A., Zaiat, A., Becker-Dombrowsky, F. M., Puchtler, S., and Kirchner, E. (2022). Investigation of the voltage-induced damage progression on the raceway surfaces of thrust ball bearings. *Machines* 10 (10), 832. doi:10.3390/machines10100832

He, F., Xie, G., and Luo, J. (2020). Electrical bearing failures in electric vehicles. *Friction* 8, 4–28. doi:10.1007/s40544-019-0356-5

Huan, J., Li, S., Xia, Z., Wang, Y., Wang, W., and Shi, G. (2022). Experimental study on electric corrosion damage of bearing and solution. *Proc. Institution Mech. Eng. Part C J. Mech. Eng. Sci.* 236 (19), 10349–10358. doi:10.1177/09544062221100328

Somani, A., Gupta, R. K., Mohapatra, K. K., and Mohan, N. (2012). On the causes of circulating currents in PWM drives with open-end winding AC machines. *IEEE Trans. industrial Electron.* 60 (9), 3670–3678. doi:10.1109/tie.2012.2208430

Suzumura, J. (2016). Prevention of electrical pitting on rolling bearings by electrically conductive grease. *Q. Rep. RTRI* 57 (1), 42–47. doi:10.2219/rtriqr.57.1_42

Tischmacher, H., Gattermann, S., Kriese, M., and Wittek, E. (2010). "Bearing wear caused by converter-induced bearing currents," in Proceedings of the IECON 2010-36th Annual Conference on IEEE Industrial Electronics Society, Glendale, Arizona, USA, November, 2010, 784–791.